Correspondence

Antiplane Piezoelectric Surface Waves over a Ceramic Half-Space with an Imperfectly Bonded Layer

Hui Fan, Jiashi Yang, *Member, IEEE*, and Limei Xu

***Abstract*—We study surface wave propagation over a piezoelectric half-space with an imperfectly bonded mass layer. The imperfect interface between the half-space and the layer is described by the so-called shear-lag model with an elastic constant characterizing the interface physical property. An analytical solution is obtained. Discussion and numerical solutions are presented.**

I. Introduction

A half-space carrying on its surface a layer of another material is a typical structure for surface acoustic wave (SAW) devices [1], [2]. In the analyses of these devices, perfect bonding between the half-space and the layer is routinely assumed, i.e., the displacement and traction are continuous across the interface between the half-space and the layer. It recently was pointed out that mass layers on crystal devices may not follow the crystal surface perfectly, and little is known about this phenomenon [3]. In addition, sometimes a very thin layer of a glue is used that has its own physical properties. Although there are mechanics models for describing an imperfect interface [4]–[6], the models mainly have been used in static analyses, and their implications in acoustic wave devices are not clear. Recently, a theoretical analysis was given on a thickness-shear bulk acoustic wave (BAW) resonator with imperfectly bonded mass layers [7]. The results in [7] show that the resonant frequencies are sensitive to the nature of the bonding, as suggested by earlier analyses from simpler models of crystal resonators with an elastically attached single particle [8], [9]. In this paper, we analyze surface waves in a ceramic half-space carrying a layer of another material. The interface is modeled by the shear-lag model [4], [5] for imperfect bonding. An analytical solution is obtained that provides new physical insights into the problem. The mathematical formulation is given in Section II. A surface wave solution is obtained in Section III, followed by discussions and numerical results in Section IV. Some conclusions are drawn in Section V.

Manuscript received February 13, 2006; accepted April 6, 2006.

H. Fan is with the School of Mechanical and Aerospace Engineering, Nanyang Technological University, Singapore 639798, Republic of Singapore.

J. Yang is with the Key Laboratory for Advanced Materials and Rheological Properties of Ministry of Education, Xiangtan University, Xiangtan, Hunan 411105, China.

J. Yang is also with the Department of Engineering Mechanics, University of Nebraska, Lincoln, NE 68588-0526 (e-mail: jyang1@unl.edu).

L. Xu is with the School of Mechtronic Engineering, University of Electronic Science and Technology of China, Chengdu, P.R. China.

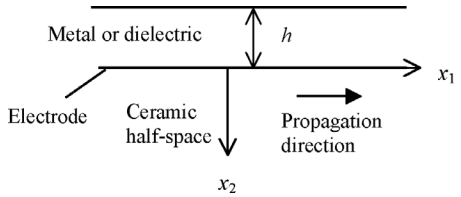

Fig. 1. An elastic layer on a ceramic half-space.

II. Formulation

Consider a ceramic half-space with a layer (see Fig. 1). The ceramic is poled along the x_3 direction. There is an ideal electrode at the interface that is grounded. On the electrode, the electric potential has to vanish. The layer is of either a metal or an isotropic (nonpiezoelectric) dielectric.

In the ceramic half-space, for antiplane motions, the displacement vector and the electric potential are given by $u_1 = u_2 = 0$, $u_3 = u(x_1, x_2, t)$, and $\phi = \phi(x_1, x_2, t)$. A function ψ can be introduced through $\phi = \psi + (e/\varepsilon)u$, where $e = e_{15}$ and $\varepsilon = \varepsilon_{11}$ are the relevant piezoelectric and dielectric constants. The governing equations for u and ψ in the half-space and u in the layer are [10], [11]:

$$\begin{aligned} &\overline{c}\nabla^2 u = \rho\ddot{u}, \quad x_2 > 0, \\ &\nabla^2\psi = 0, \quad x_2 > 0, \\ &\hat{c}\nabla^2 u = \hat{\rho}\ddot{u}, \quad -h < x_2 < 0, \end{aligned} \tag{1}$$

where ∇^2 is the two-dimensional Laplacian, $\overline{c} = c + e^2/\varepsilon$, and $c = c_{44}$ is the relevant elastic constant. $\hat{\rho}$ and $\hat{c}$ are the mass density and shear modulus of the layer. We look for surface solutions satisfying:

$$u, \psi \to 0, \quad x_2 \to +\infty. \tag{2}$$

At the free surface of $x_2 = -h$, we have traction-free boundary condition with $T_{23} = 0$. At the interface $x_2 = 0$, the electrical boundary condition is $\phi = 0$. The mechanical interaction at the interface is described by the shear-lag model and will be given in the next section.

III. Surface Wave Solution

For $x_2 > 0$, the solutions to $(1)_1$ satisfying (2) can be written as:

$$\begin{aligned} u &= A\exp(-\xi_2 x_2)\cos(\xi_1 x_1 - \omega t), \\ \psi &= B\exp(-\xi_1 x_2)\cos(\xi_1 x_1 - \omega t), \end{aligned} \tag{3}$$

where A and B are constants; $(3)_2$ already satisfies $(1)_2$. For $(3)_1$ to satisfy $(1)_1$, the following must be true:

$$\xi_2^2 = \xi_1^2 - \frac{\rho\omega^2}{\overline{c}} = \xi_1^2\left(1 - \frac{v^2}{v_T^2}\right) > 0, \tag{4}$$

where:

$$v^2 = \frac{\omega^2}{\xi_1^2}, \quad v_T^2 = \frac{\overline{c}}{\rho}. \tag{5}$$

The electric potential and the stress component needed for the boundary and continuity conditions are:

$$\begin{aligned} T_{23} &= \overline{c}u_{,2} + e\psi_{,2} \\ &= -\left[\overline{c}A\xi_2 \exp\left(-\xi_2 x_2\right)\right. \\ &\quad \left. + eB\xi_1 \exp\left(-\xi_1 x_2\right)\right] \cos\left(\xi_1 x_1 - \omega t\right), \\ \phi &= \psi + \frac{e}{\varepsilon}u \\ &= \left[\frac{e}{\varepsilon}A\exp\left(-\xi_2 x_2\right) + B\exp\left(-\xi_1 x_2\right)\right]\cos\left(\xi_1 x_1 - \omega t\right). \end{aligned} \tag{6}$$

For $-h < x_2 < 0$, we write:

$$u = \left(\hat{A}\cos\hat{\xi}_2 x_2 + \hat{B}\sin\hat{\xi}_2 x_2\right)\cos\left(\xi_1 x_1 - \omega t\right), \tag{7}$$

where:

$$\hat{\xi}_2^2 = \frac{\hat{\rho}\omega^2}{\hat{c}} - \xi_1^2 = \xi_1^2\left(\frac{v^2}{\hat{v}_T^2} - 1\right), \tag{8}$$

and:

$$\hat{v}_T^2 = \frac{\hat{c}}{\hat{\rho}}. \tag{9}$$

For boundary conditions, we need:

$$\begin{aligned} &T_{23} = \hat{c}u_{,2} = \\ &\hat{c}\left(-\hat{A}\hat{\xi}_2\sin\hat{\xi}_2 x_2 + \hat{B}\hat{\xi}_2\cos\hat{\xi}_2 x_2\right)\cos\left(\xi_1 x_1 - \omega t\right). \end{aligned} \tag{10}$$

The continuity and boundary conditions are [except for a factor of $\cos\left(\xi_1 x_1 - \omega t\right)$]:

$$\begin{aligned} &\phi(0^+) = \frac{e}{\varepsilon}A + B = 0, \\ &T_{23}(0^+) = -\overline{c}A\xi_2 - eB\xi_1 = \hat{c}\hat{B}\hat{\xi}_2 = T_{23}(0^-), \\ &T_{23} = K\left(u(0^+) - u(0^-)\right), \\ &T_{23}(-h) = \hat{c}\left(\hat{A}\hat{\xi}_2\sin\hat{\xi}_2 h + \hat{B}\hat{\xi}_2\cos\hat{\xi}_2 h\right) = 0, \end{aligned} \tag{11}$$

where $(11)_3$ represents the shear-lag model [4], [5]. The model describes an elastic interface with K as the elastic or spring constant. With this model, the interface is allowed to deform, and the displacement at the interface is no longer continuous. In the special case when $K \to \infty$, a perfect interface is recovered. Using $(11)_{1,3}$ to eliminate A and B, we obtain:

$$\begin{aligned} &\overline{c}\left(\frac{e^2}{\overline{c}\varepsilon}\xi_1 - \xi_2\right)\hat{A} - \hat{c}\left[\left(\frac{e^2}{\overline{c}\varepsilon}\xi_1 - \xi_2\right)\frac{\overline{c}\hat{\xi}_2}{K} - \hat{\xi}_2\right]\hat{B} = 0, \\ &\hat{A}\sin\hat{\xi}_2 h + \hat{B}\cos\hat{\xi}_2 h = 0. \end{aligned} \tag{12}$$

For nontrivial solutions, the determinant of the coefficient matrix has to vanish, i.e.:

$$\frac{\xi_2}{\xi_1} - \frac{\hat{c}}{\overline{c}}\frac{\hat{\xi}_2}{\xi_1}\left[1 - \frac{\overline{c}\hat{\xi}_2}{K}\left(\overline{k}^2 - \frac{\xi_2}{\xi_1}\right)\right]\tan\hat{\xi}_2 h = \overline{k}^2 = \frac{e^2}{\varepsilon\overline{c}}. \tag{13}$$

Substituting from (4) and (8), we obtain (14) (see next page), which determines the surface wave speed v as a function of the wave number ξ_1. Therefore, the waves are dispersive.

IV. Discussion and Numerical Results

We make the following observations from (14):

A. Bleustein-Gulyaev Wave

When $h = 0$, (14) reduces to:

$$\sqrt{1 - \frac{v^2}{v_T^2}} = \overline{k}^2, \tag{15}$$

or:

$$v^2 = v_T^2\left(1 - \overline{k}^4\right), \tag{16}$$

which is the well-known Bleustein-Gulyaev wave over a ceramic half-space with an electroded surface [10], [12].

B. Perfect Bonding

When $K \to \infty$, the layer is perfectly bonded to the half-space, and (14) reduces to:

$$\sqrt{1 - \frac{v^2}{v_T^2}} - \frac{\hat{c}}{\overline{c}}\sqrt{\frac{v^2}{\hat{v}_T^2} - 1}\tan\left[\xi_1 h\sqrt{\frac{v^2}{\hat{v}_T^2} - 1}\right] = \overline{k}^2, \tag{17}$$

which is the result of [13]. If we further set $\overline{k}^2 = 0$, (17) becomes the frequency equation for Love waves in an elastic half-space carrying an elastic layer [14]. The dispersion relations for Love waves are real and multivalued when $\hat{v}_T^2 < v^2 < v_T^2$, for which the elastic shear wave speed of the layer has to be smaller than that of the half-space. In other words, the half-space is more shear-rigid than the layer.

C. Unbonded Layer

When $K = 0$, the mechanical interaction at the interface disappears, and (14) reduces to (18) (see next page).

Eq. (18) has four factors. The first and the second are the same, and they simply imply:

$$v = \hat{v}_T, \tag{19}$$

which is the face-shear wave [an antiplane or shear horizontal (SH) plate wave] in the layer [14]. The third factor

$$\sqrt{1-\frac{v^2}{v_T^2}}-\frac{\hat{c}}{\overline{c}}\sqrt{\frac{v^2}{\hat{v}_T^2}-1}\left[1-\frac{\overline{c}}{K}\xi_1\sqrt{\frac{v^2}{\hat{v}_T^2}-1}\left(\overline{k}^2-\sqrt{1-\frac{v^2}{v_T^2}}\right)\right]\tan\left[\xi_1 h\sqrt{\frac{v^2}{\hat{v}_T^2}-1}\right]=\overline{k}^2, \tag{14}$$

$$-\frac{\hat{c}}{\overline{c}}\sqrt{\frac{v^2}{\hat{v}_T^2}-1}\left[-\overline{c}\xi_1\sqrt{\frac{v^2}{\hat{v}_T^2}-1}\left(\overline{k}^2-\sqrt{1-\frac{v^2}{v_T^2}}\right)\right]\tan\left[\xi_1 h\sqrt{\frac{v^2}{\hat{v}_T^2}-1}\right]=0. \tag{18}$$

yields (15) or (16) for Bleustein-Gulyaev waves. The fourth factor of (18) gives:

$$\tan\left[\xi_1 h\sqrt{\frac{v^2}{\hat{v}_T^2}-1}\right]=0, \tag{20}$$

which determines thickness-twist waves (antiplane or SH plate waves) of the layer [14].

D. Nonpiezoelectric Material

When the electromechanical coupling factor $\overline{k}=0$, (14) reduces to (21) (see next page), which determines elastic surfaces waves in a half-space with an imperfectly bonded layer. This special result appears to be new.

E. Long Waves

In applications we often encounter long waves with a wavelength much larger than the layer thickness ($\xi_1 h \ll 1$). We examine the effects of K on long waves below. For small $\xi_1 h$, (14) can be approximated by (22) (see next page), where the dimensionless parameters, α, β, and γ are defined as:

$$\alpha=\frac{\hat{c}}{\overline{c}},\quad \beta=\frac{v_T^2}{\hat{v}_T^2}=\frac{\overline{c}\hat{\rho}}{\rho\hat{c}},\quad \gamma=\frac{\overline{c}}{Kh}. \tag{23}$$

We perform some numerical calculations from (22). For the piezoelectric half-space, we use PZT-5H with $c=c_{44}=2.3\times10^{10}$ N/m^2, $\rho=7500$ kg/m^3, $e=e_{15}=17$ C/m^2, and $\varepsilon=1.505$ C/Vm [11]. Then:

$$k^2=\frac{e^2}{c\varepsilon}=0.8377,\quad \overline{k}^2=\frac{e^2}{\overline{c}\varepsilon}=0.4558. \tag{24}$$

For the layer, we examine the two cases of gold and aluminum layers. They are common electrode materials, and the layer can represent an electrode with a thickness that cannot be neglected. The material constants of gold and aluminum are listed in Table I. The nondimensional constant α and β are also listed in Table I.

Fig. 2 shows the case for a gold layer with $\beta>1$. Two roots are expected from (22), representing the Bleustein-Gulyaev wave and Love wave, respectively. In the long wave range shown, only one root is present. Its speed suggests it is a Bleustein-Gulyaev wave modified by a layer with a thickness, and hence it has become dispersive. The three curves are for a perfect interface ($\gamma=0$) and $\gamma=1$ and 10. The curves are close; therefore, $\gamma=1$ and 10 may be considered as cases of almost perfect bonding. Fig. 2 shows that imperfection reduces the wave speed. This is because, when compared to the case of perfect interface with $\gamma=0$ which is shear-rigid, the cases for $\gamma=1$ and 10 represent a shear-deformable interface with less stiffness, and therefore, lower frequency or wave speed.

TABLE I
MATERIAL CONSTANTS OF METAL LAYERS ON PZT-5H.

Metal layer	Shear modulus	Density	α	β
Gold	30 Gpa	19.3 Mg/m^3	0.71	3.6
Aluminum	27 Gpa	2.7 Mg/m^3	0.64	0.56

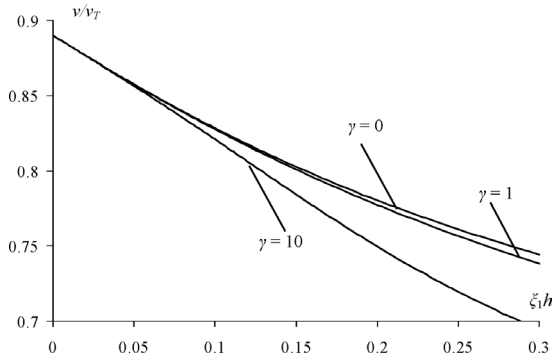

Fig. 2. Dispersion relations for a gold layer on PZT-5H (small γ, near perfect bonding).

Fig. 3 is still for a gold layer, but it is for larger values of $\gamma=100$ and 1000. They represent the cases of relatively loosely bonded interfaces. In this case, two real roots of (22) can be found in the range shown. The two branches of the dispersion relations for Love waves are bounded from above by $v/v_T<1$ [14]. The wave speeds are reduced by the increases of the interface imperfection.

For an aluminum layer on PZT-5H, we have $\beta<1$. In this case, Love wave does not exist [14]. No solution is found from (22) when the interface is imperfect. However, when $\gamma=0$ (perfect interface), a solution can be found and is compared with the case of a gold layer in Fig. 4. It was shown recently that a layer affects the frequency or wave speed through both of the layer inertia, which lowers the speed and the layer stiffness that raises the speed

$$\sqrt{1-\frac{v^2}{v_T^2}}-\frac{\hat{c}}{\overline{c}}\sqrt{\frac{v^2}{\hat{v}_T^2}-1}\left[1-\frac{\overline{c}}{K}\xi_1\sqrt{\frac{v^2}{\hat{v}_T^2}-1}\left(-\sqrt{1-\frac{v^2}{v_T^2}}\right)\right]\tan\left[\xi_1 h\sqrt{\frac{v^2}{\hat{v}_T^2}-1}\right]=0, \tag{21}$$

$$\sqrt{1-\frac{v^2}{v_T^2}}-\alpha\left(\beta\frac{v^2}{v_T^2}-1\right)\left[1-\gamma\xi_1 h\sqrt{\beta\frac{v^2}{v_T^2}-1}\left(\overline{k}^2-\sqrt{1-\frac{v^2}{v_T^2}}\right)\right]\xi_1 h=\overline{k}^2, \tag{22}$$

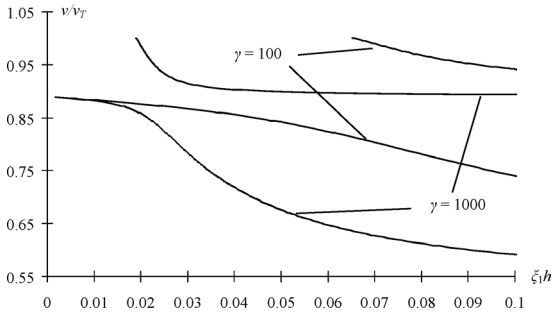

Fig. 3. Dispersion relations for a gold layer on PZT-5H (large γ, loose bonding).

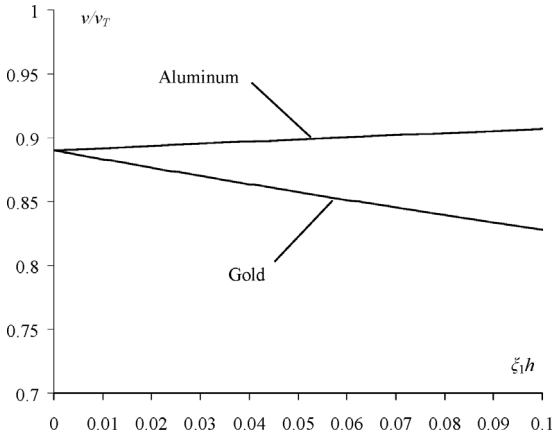

Fig. 4. Dispersion relations for different metal layers with perfect bonding.

[15]. This explains the interesting result in Fig. 4. For gold, which is heavy, the inertial effect dominates, and the frequency is lowered. For aluminum, which is relatively light, the stiffness effect dominates, and the frequency becomes higher. This is a more comprehensive picture of the effect of a layer on wave speed. It shows that the usual understanding of the reduction of wave speed due to layer inertia is not complete. The layer stiffness also may be important.

V. Conclusions

An exact solution for antiplane waves in a ceramic half-space with an imperfectly bonded layer is obtained. The solution generalizes a few known results and includes them as special cases. Numerical results show that the dispersion relations of the waves are sensitive to the interface property. In the examples analyzed, the interface imperfection lowers the wave speed. The results are useful for understanding the behavior of waves in a half-space with a mass layer.

References

[1] E. Benes, M. Gröschl, W. Burger, and M. Schmid, "Sensors based on piezoelectric resonators," *Sens. Actuators A*, vol. 48, pp. 1–21, 1995.

[2] R. M. Lec, "Piezoelectric biosensors," in *Proc. IEEE Int. Freq. Contr. Symp. PDA Exhibition*, 2001, pp. 419–429.

[3] J. R. Vig and A. Ballato, "Comments about the effects of nonuniform mass loading on a quartz crystal microbalance," *IEEE Trans. Ultrason., Ferroelect., Freq. Contr.*, vol. 45, pp. 1123–1124, 1998.

[4] Z.-Q. Cheng, A. K. Jemah, and F. W. Williams, "Theory for multilayered anisotropic plates with weakened interfaces," *Amer. Soc. Mech. Eng. J. Appl. Mech.*, vol. 63, pp. 1019–1026, 1996.

[5] U. A. Handge, "Analysis of a shear-lag model with nonlinear elastic stress transfer for sequential cracking of polymer coatings," *J. Mater. Sci.*, vol. 37, pp. 4775–4782, 2002.

[6] F. Ferrante and A. L. Kipling, "Molecular slip at the solid-liquid interface of an acoustic-wave sensor," *J. Appl. Phys.*, vol. 76, pp. 3448–3462, 1994.

[7] J. S. Yang, Y. T. Hu, Y. Zeng, and H. Fan, "Thickness-shear vibrations of rotated y-cut quartz plates with imperfectly bonded surface mass layers," *IEEE Trans. Ultrason., Ferroelect., Freq. Contr.*, vol. 53, pp. 241–245, 2006.

[8] G. L. Dybwad, "A sensitive new method for the determination of adhesive bonding between a particle and a substrate," *J. Appl. Phys.*, vol. 58, pp. 2789–2790, 1985.

[9] L. Dworsky, "A simple single model for quartz crystal resonator low level drive sensitivity and monolithic filter intermodulation," *IEEE Trans. Ultrason., Ferroelect., Freq. Contr.*, vol. 41, pp. 261–268, 1994.

[10] J. L. Bleustein, "A new surface wave in piezoelectric materials," *Appl. Phys. Lett.*, vol. 13, pp. 412–413, 1968.

[11] J. S. Yang, *An Introduction to the Theory of Piezoelectricity*. New York: Springer, 2005.

[12] Y. V. Gulyaev, "Electroacoustic surface waves in solids," *Sov. Phys. JETP Lett.*, vol. 9, pp. 37–38, 1969.

[13] R. G. Curtis and M. Redwood, "Transverse surface waves on a piezoelectric material carrying a metal layer of finite thickness," *J. Appl. Phys.*, vol. 44, pp. 2002–2007, 1973.

[14] K. F. Graff, *Wave Motion in Elastic Solids*. New York: Dover, 1991.

[15] J. S. Yang and S. H. Guo, "Frequency shifts in a piezoelectric body due to a surface mass layer with consideration of the layer stiffness," *IEEE Trans. Ultrason., Ferroelect., Freq. Contr.*, vol. 52, pp. 1200–1203, 2005.